assistance. This work was supported by the Ministry of Health, Labour, and Welfare of Japan (24133701,11103577, 11103340 and 10103235); a Grant-in-Aid for Scientific Research (C) from the Japan Society for the Promotion of Science (24591500); a Grant-in-Aid for Young Scientists from the Japan Society for the Promotion of Science (10013428 and 12020465); the Takeda Science Foundation; the Japan Science and Technology Agency; the Strategic Research Program for Brain Sciences (11105137); and a Grant-in-Aid for Scientific Research on Innovative Areas (Transcription Cycle) from the Ministry of Education, Culture, Sports, Science, and Technology of Japan (12024421).

K Nakamura[a,b]
M Kato[b]
J Tohyama[c]
T Shiohama[d]
K Hayasaka[b]
K Nishiyama[a]
H Kodera[a]
M Nakashima[a]
Y Tsurusaki[a]
N Miyake[a]
N Matsumoto[a]
H Saitsu[a]

[a]Department of Human Genetics
Yokohama City University Graduate School of Medicine
Yokohama, Japan
[b]Department of Pediatrics
Yamagata University Faculty of Medicine
Yamagata, Japan
[c]Department of Pediatrics
Epilepsy Center, Nishi-Niigata Chuo National Hospital
Niigata, Japan
[d]Department of Pediatrics
Kimitsu Chuo Hospital
Chiba, Japan

References

1. Mirzaa GM, Conway RL, Gripp KW et al. Megalencephaly-capillary malformation (MCAP) and megalencephaly-polydactyly-poly microgyria-hydrocephalus (MPPH) syndromes: two closely related disorders of brain overgrowth and abnormal brain and body morphogenesis. Am J Med Genet A 2012: 158A: 269–291.
2. Riviere JB, Mirzaa GM, O'Roak BJ et al. De novo germline and postzygotic mutations in *AKT3*, *PIK3R2* and *PIK3CA* cause a spectrum of related megalencephaly syndromes. Nat Genet 2012: 44: 934–940.
3. Franke TF. PI3K/Akt: getting it right matters. Oncogene 2008: 27: 6473–6488.
4. Tohyama J, Akasaka N, Saito N, Yoshimura J, Nishiyama K, Kato M. Megalencephaly and polymicrogyria with polydactyly syndrome. Pediatr Neurol 2007: 37: 148–151.
5. Liu BA, Jablonowski K, Raina M, Arcé M, Pawson T, Nash PD. The human and mouse complement of SH2 domain proteins – establishing the boundaries of phosphotyrosine signaling. Mol Cell 2006: 22: 851–868.
6. Lee JH, Huynh M, Silhavy JL et al. De novo somatic mutations in components of the PI3K-AKT3-mTOR pathway cause hemimegalencephaly. Nat Genet 2012: 44: 941–945.
7. Poduri A, Evrony GD, Cai X et al. Somatic activation of AKT3 causes hemispheric developmental brain malformations. Neuron 2012: 74: 41–48.
8. Lindhurst MJ, Sapp JC, Teer JK et al. A mosaic activating mutation in *AKT1* associated with the Proteus syndrome. N Engl J Med 2011: 365: 611–619.

Correspondence:
Dr Kazuyuki Nakamura, MD
Department of Pediatrics
Yamagata University Faculty of Medicine
2-2-2 Iida-nishi
Yamagata 990-9585
Japan
Tel: +81-23-628-5329
Fax: +81-23-628-5331
e-mail: kazun-yamagata@umin.ac.jp

ELSEVIER

Brain & Development xxx (2013) xxx–xxx

BRAIN & DEVELOPMENT
Official Journal of the Japanese Society of Child Neurology

www.elsevier.com/locate/braindev

Case report

Compound heterozygosity in *GPR56* with bilateral frontoparietal polymicrogyria

Yuji Fujii [a,*], Nobutsune Ishikawa [a], Yoshiyuki Kobayashi [a], Masao Kobayashi [a], Mitsuhiro Kato [b]

[a] *Department of Pediatrics, Hiroshima University Hospital, Hiroshima, Japan*
[b] *Department of Pediatrics, Yamagata University, Faculty of Medicine, Yamagata, Japan*

Received 24 May 2013; received in revised form 28 July 2013; accepted 31 July 2013

Abstract

Polymicrogyria is caused by a diverse etiology, one of which is gene mutation. At present, only one gene (*GPR56*) is known to cause polymicrogyria, which leads to a distinctive phenotype termed bilateral frontoparietal polymicrogyria (BFPP). BFPP is an autosomal recessive inherited human brain malformation with abnormal cortical lamination. Here, we identified compound heterozygous *GPR56* mutations in a patient with BFPP. The proband was a Japanese female born from non-consanguineous parents. She presented with mental retardation, developmental motor delay, epilepsy exhibiting the feature of Lennox–Gastaut syndrome, exotropia, bilateral polymicrogyria with a relatively spared perisylvian region, bilateral patchy-white-matter MRI signal changes, and hypoplastic pontine basis. *GPR56* sequence analysis revealed a c.107G>A substitution leading to a p.S36N, and a c.113G>A leading to a p.R38Q. Although affected individuals with compound heterozygosity in *GPR56* have not been previously described, we presume that compound heterozygosity of these two mutations in a ligand binding domain within the extracellular N-terminus of protein could result in BFPP. In addition, we observed unusually less involvement of perisylvian cortex for polymicrogyria, and Lennox–Gastaut syndrome for epilepsy, which are likely common features in patients with BFPP caused by *GPR56* mutations.

Keywords: Polymicrogyria; Lennox–Gastaut; GPR56; Heterozygous mutation

1. Introduction

The autosomal recessive bilateral frontoparietal polymicrogyria (BFPP) is a well-characterized neuronal migration defect that shows bilateral polymicrogyria with an anterior to posterior gradient, bilateral patchy-white-matter MRI signal changes (without specific patterns), and brainstem or cerebellar hypoplasia. Patients with BFPP present with mental retardation, developmental motor delay, seizures, ataxia, and dysconjugate gaze [1]. The causative gene for BFPP is the G protein-coupled receptor 56 gene (*GPR56*) [2]. GPR56 is one of the adhesion G protein-coupled receptors (GPCRs). Like other members of the adhesion GPCRs, GPR56 has an unusually long N-terminal extracellular domain that contains a high percentage of serine and threonine residues and a GPCR proteolytic site domain just before the first transmembrane spanning domain [3,4]. The serine and threonine-rich region can serve as an O- and/or N-glycosylation site [3,4].

So far, multiple independent mutations have been identified in *GPR56*, all of which are homozygous germline mutations. To date, 25 mutations in *GPR56*, including nine N-terminal extracellular domain mutations, are

* Corresponding author. Address: Department of Pediatrics, Hiroshima University Hospital, Faculty of Medicine, Hiroshima University, 1-2-3 Kasumi-cho, Hiroshima 734-8551, Japan. Tel.: +81 82 257 5212; fax: +81 82 257 5214.
E-mail address: yujinn0728@ybb.ne.jp (Y. Fujii).

0387-7604/$ - see front matter
http://dx.doi.org/10.1016/j.braindev.2013.07.015

Please cite this article in press as: Fujii Y et al. Compound heterozygosity in *GPR56* with bilateral frontoparietal polymicrogyria. Brain Dev (2013), http://dx.doi.org/10.1016/j.braindev.2013.07.015

reported in humans [1,2,5–8]. Here we report a BFPP patient carrying compound heterozygous mutations with a novel *GPR56* mutation, p.S36Q, and a previously reported mutation, p.R38Q. Additionally, we review previous reports and discuss the radiological and clinical features of BFPP patients.

2. Case report

The proband was a Japanese female born from non-consanguineous parents. She had normal prenatal and perinatal histories and normal head growth, but showed developmental delay within the first year of life. Complex partial seizures occurred at 2 months; carbamazepine was effective for the seizures. Since the age of two years, epileptic spasms in clusters have appeared and have been refractory to medications. Around the age of four years, she developed tonic seizures causing drop attacks, in addition to epileptic spasms.

The seizures persisted despite treatment with multiple antiepileptic drugs. Interictal electroencephalogram (EEG) showed generalized bursts of sharp waves and slow spike-wave discharges with anterior predominance (Fig. 1). Video-EEG monitoring (Grass Technology, West Warwick, RI, USA) at 6 years old revealed that she suffered from frequent atypical absence seizures and tonic seizures. She was diagnosed with Lennox–Gastaut syndrome by specific EEG features and seizures. At this age, she had moderate to severe developmental delay (developmental quotient = DQ: 33). She was unable to walk without help, and her speech was limited to a few isolated words. Neurologic examination revealed mild spasticity, hyperactive deep-tendon reflexes, poor coordination, and exotropia. She showed neither dysmorphic features nor other congenital anomalies.

Brain MRI at 6 years of age revealed bilateral polymicrogyria with an anterior to posterior gradient, in contrast to the relatively spared perisylvian regions, patchy signal change in the bilateral white matter, hypoplastic pons, and multiple small cysts in the corpus callosum (Fig. 2).

2.1. Mutation analysis

DNA was extracted from peripheral blood leukocytes obtained from the patient and her parents using standard methods, and after obtaining informed consent from the parents. We performed a mutation screening of for all coding exons and flanking introns of *GPR56* using the high-resolution melt analysis (HRM) or capillary sequencing. PCR samples showing an aberrant melting curve pattern were sequenced. PCR primers and conditions are available on request.

Mutation analysis revealed a compound heterozygous mutation in exon 2 of*GPR56,* (c.107G>A and c.113G>A), (which presumably leads to amino acid changes), (p.S36N and p.R38Q, respectively) in the extracellular N-terminus of the protein. Her father was heterozygous for the p.S36N mutation, and her mother carried the p.R38Q mutation, which indicates an autosomal recessive inheritance (Fig. 3). Both changes were not found in one individual among 80 Japanese controls.

3. Discussion

BFPP is an autosomal recessive polymicrogyria syndrome, which was frequently underdiagnosed before genetic testing and high-resolution neuroimaging were available.

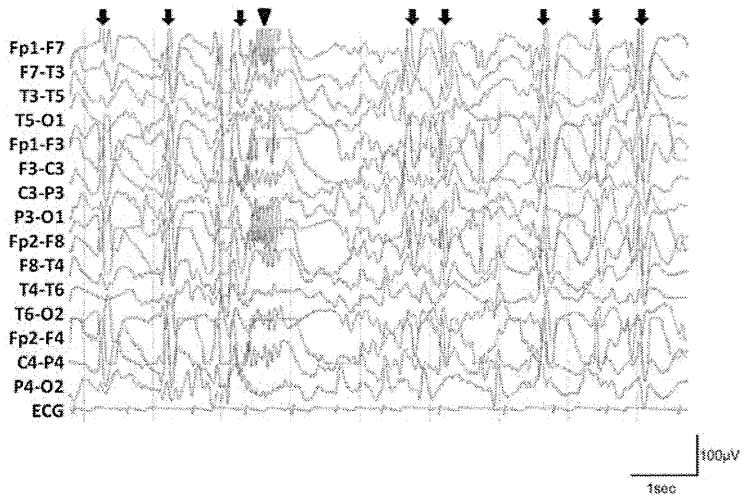

Fig. 1. Electroencephalography (EEG) finding. Generalized bursts of sharp waves (arrow head) and slow spike-wave discharges (arrows) with anterior predominance were seen during sleep.

Please cite this article in press as: Fujii Y et al. Compound heterozygosity in *GPR56* with bilateral frontoparietal polymicrogyria. Brain Dev (2013), http://dx.doi.org/10.1016/j.braindev.2013.07.015

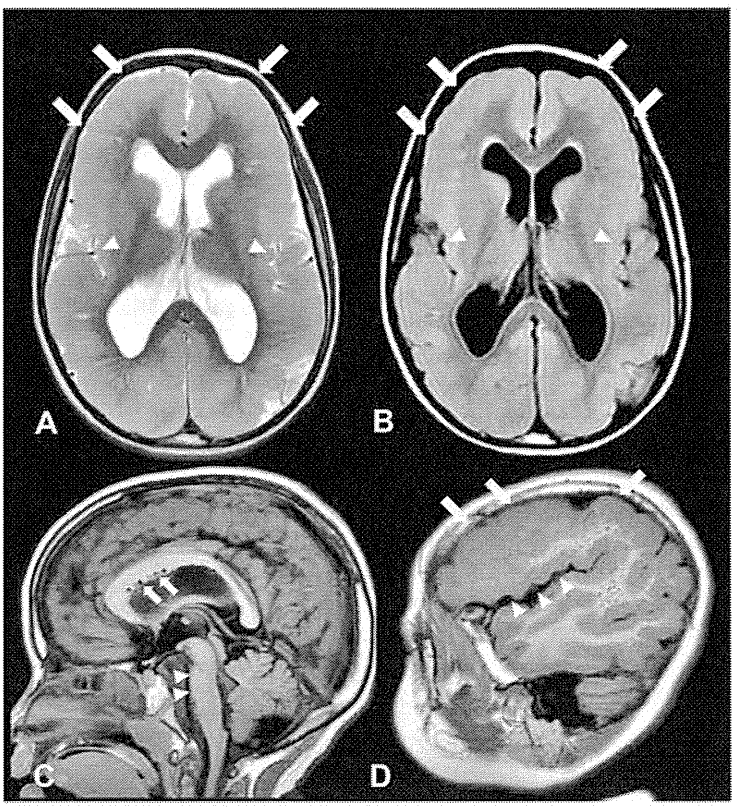

Fig. 2. Neuroimaging. Axial T2WI (A) and FLAIR (B) images demonstrate bilaterally symmetric thick cortex and irregular gyri compatible to polymicrogyria with anterior to posterior gradient (arrows) and, patchy high signals on both T2WI and FLAIR in the frontal subcortical white matter. Note the less involved insular cortex (arrow heads). Sagittal T1WI (C) shows flat pontine basis (arrow heads) and small cystic lesions in the corpus callosum (arrows). Sagittal T1WI (D) shows bilateral polymicrogyria with anterior to posterior gradient (arrows), in contrast with relatively spared perisylvian region (arrow heads).

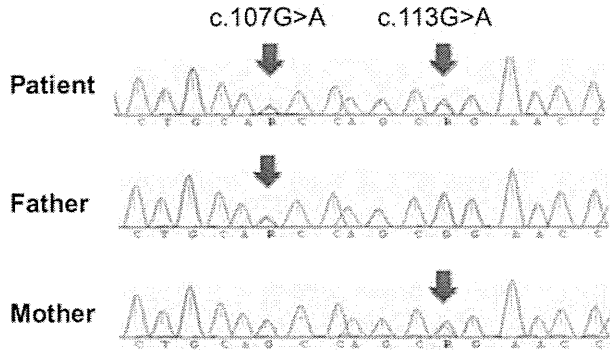

Fig. 3. Mutation analysis. Sequence chromatograms showing segregation of the compound heterozygous c.107G>A and c. 113G>A mutations in *GPR56* in the patient and her parents.

Piao, et al. [2] reported that the clinical phenotype of BFPP patients harboring *GPR56* mutations show considerable clinical homogeneity. This included five common clinical features and three typical MRI findings: (1) mental retardation of moderate to severe degree; (2) motor development delay; (3) seizures, most commonly symptomatic generalized epilepsy; (4) cerebellar signs, consisting of ataxia; (5) dysconjugate gaze, presenting variably as esotropia, nystagmus, exotropia, or strabismus; (6) bilateral polymicrogyria with anterior to posterior gradient; (7) bilateral patchy-white-matter signal changes without specific pattern; and (8) brain stem and cerebellar hypoplasia [1]. Thus, according to this description, our patient demonstrates the cardinal features of BFPP. Polymicrogyria typically has a predilection for the perisylvian cortex [9]. Our patient, however, shows less involvement of the perisylvian cortex, compared to the other regions where lesions were observed. Frontoparietal distribution of polymicrogyria is the most common feature of BFPP, but some patients show extensive distribution throughout the entire brain, as was observed with our patient [5,10]. Although other previous reports do not describe perisylvian cortex findings in detail, less involvement of perisylvian cortex might be a feature of BFPP caused by a GPR56 mutation.

Epilepsy is a common clinical problem in patients with BFPP caused by *GPR56* mutations [1,5–8,10]. Similar to our patient, four affected individuals from three families with BFPP caused by *GPR56* mutations had

Please cite this article in press as: Fujii Y et al. Compound heterozygosity in *GPR56* with bilateral frontoparietal polymicrogyria. Brain Dev (2013), http://dx.doi.org/10.1016/j.braindev.2013.07.015

Lennox–Gastaut syndrome [6]. Lennox–Gastaut syndrome manifestations can occur among patients with BFPP caused by GPR56 mutations.

Our patient had a compound heterozygous mutation of*GPR56* (p.S36N and p.R38Q), whereas other patients with BFPP have homozygous mutations of *GPR56* [1,2,5–8]. Both mutations are located in the ligand binding domain within the extracellular N-terminus of the protein, as was observed in the nine previously reported ligand binding domain mutations [1,2,5,6,8]. A homozygous p.R38Q mutation never has been reported with BFPP [1]. Moreover, a detailed analysis of the biochemical modifications by *GPR56* revealed that the disease-associated *GPR56* missense mutations in the tip of the N-terminal domain (p.R38Q) produced proteins with reduced intracellular trafficking and poor cell surface expression [11]. Similar to p.R38Q, p.S36N is another substitution and a novel mutation that locates a ligand binding domain within the extracellular N-terminus of the protein. Compound heterozygosity of these two mutations in the ligand binding domain could impair the subcellular trafficking of the GPR56 receptor, and reduce its cell surface expression, leading to BFPP.

Acknowledgments

This study was supported by the Health and Labour Sciences Research Grant from the Ministry of Health, Labour and Welfare of Japan (25140101) and a Grant-in-Aid for Scientific Research (C) from the Japan Society for the Promotion of Science (24591500) to M Kato. We thank Keiko Tanaka, Yamagata University, for providing technical assistance.

References

[1] Piao X, Chang BS, Bodell A, Woods K, Benzeev B, Topcu M, et al. Genotype–phenotype analysis of human frontoparietal polymicrogyria syndromes. Ann Neurol 2005;58:680–7.
[2] Piao X, Hill RS, Bodell A, Chang BS, Basel-Vanagaite L, Straussberg R, et al. G protein-coupled receptor-dependent development of human frontal cortex. Science 2004;303:2033–6.
[3] Stacey M, Lin HH, Gordon S, McKnight AJ. LNB-TM7, a group of seven-transmembrane proteins related to family-B G-protein-coupled receptors. Trends Biochem Sci 2000;25:284–9.
[4] Bjarnadóttir TK, Fredriksson R, Höglund PJ, Gloriam DE, Lagerström MC, Schiöth HB. The human and mouse repertoire of the adhesion family of G-protein-coupled receptors. Genomics 2004;84(1):23–33.
[5] Bahi-Buisson N, Poirier K, Boddaert N, Fallet-Bianco C, Specchio N, Bertini E, et al. GPR56-related bilateral frontoparietal polymicrogyria: further evidence for an overlap with the cobblestone complex. Brain 2010;133:3194–209.
[6] Parrini E, Ferrari AR, Dorn T, Walsh CA, Guerrini R. Bilateral frontoparietal polymicrogyria, Lennox–Gastaut syndrome, and GPR56 gene mutations. Epilepsia 2009;50:1344–53.
[7] Luo R, Yang HM, Jin Z, Halley DJ, Chang BS, MacPherson L, et al. A novel GPR56 mutation causes bilateral frontoparietal polymicrogyria. Pediatr Neurol 2011;45:49–53.
[8] Quattrocchi CC, Zanni G, Napolitano A, Longo D, Cordelli DM, et al. Conventional magnetic resonance imaging and diffusion tensor imaging studies in children with novel GPR56 mutations: further delineation of a cobblestone-like phenotype. Neurogenetics 2013;14:77–83.
[9] Leventer RJ, Jansen A, Pilz DT, Stoodley N, Marini C, Dubeau F, et al. Clinical and imaging heterogeneity of polymicrogyria: a study of 328 patients. Brain 2010;133:1415–27.
[10] Chang BS, Piao X, Bodell A, Basel-Vanagaite L, Straussberg R, Dobyns WB, et al. Bilateral frontoparietal polymicrogyria: clinical and radiological features in 10 families with linkage to chromosome 16. Ann Neurol 2003;53:596–606.
[11] Jin Z, Tietjen I, Bu L, Liu-Yesucevitz L, Gaur SK, Walsh CA, et al. Disease-associated mutations affect GPR56 protein trafficking and cell surface expression. Hum Mol Genet 2007;16:1972–85.

Please cite this article in press as: Fujii Y et al. Compound heterozygosity in *GPR56* with bilateral frontoparietal polymicrogyria. Brain Dev (2013). http://dx.doi.org/10.1016/j.braindev.2013.07.015

Phenotypic Spectrum of *COL4A1* Mutations: Porencephaly to Schizencephaly

Yuriko Yoneda, MSc,[1] Kazuhiro Haginoya, MD, PhD,[2,3] Mitsuhiro Kato, MD, PhD,[4] Hitoshi Osaka, MD, PhD,[5] Kenji Yokochi, MD, PhD,[6] Hiroshi Arai, MD,[7] Akiyoshi Kakita, MD, PhD,[8] Takamichi Yamamoto, MD, MS, DMSc,[9] Yoshiro Otsuki, MD, PhD,[10] Shin-ichi Shimizu, DDS, PhD,[10] Takahito Wada, MD, PhD,[5] Norihisa Koyama, MD, PhD,[11] Yoichi Mino, MD,[12] Noriko Kondo, MD,[13] Satoru Takahashi, MD, PhD,[14] Shinichi Hirabayashi, MD, PhD,[15] Jun-ichi Takanashi, MD, PhD,[16] Akihisa Okumura, MD, PhD,[17] Toshiyuki Kumagai, MD,[18] Satori Hirai, MD,[7] Makoto Nabetani, MD,[19] Shinji Saitoh, MD, PhD,[20] Ayako Hattori, MD, PhD,[20] Mami Yamasaki, MD, PhD,[21] Akira Kumakura, MD,[22] Yoshinobu Sugo, MD,[1] Kiyomi Nishiyama, PhD,[1] Satoko Miyatake, MD, PhD,[1] Yoshinori Tsurusaki, PhD,[1] Hiroshi Doi, MD, PhD,[1] Noriko Miyake, MD, PhD,[1] Naomichi Matsumoto, MD, PhD,[1] and Hirotomo Saitsu, MD, PhD[1]

Objective: Recently, *COL4A1* mutations have been reported in porencephaly and other cerebral vascular diseases, often associated with ocular, renal, and muscular features. In this study, we aimed to clarify the phenotypic spectrum and incidence of *COL4A1* mutations.
Methods: We screened for *COL4A1* mutations in 61 patients with porencephaly and 10 patients with schizencephaly, which may be similarly caused by disturbed vascular supply leading to cerebral degeneration, but can be distinguished depending on time of insult.
Results: *COL4A1* mutations were identified in 15 patients (21%, 10 mutations in porencephaly and 5 mutations in schizencephaly), who showed a variety of associated findings, including intracranial calcification, focal cortical dysplasia, pontocerebellar atrophy, ocular abnormalities, myopathy, elevated serum creatine kinase levels, and hemolytic anemia. Mutations include 10 missense, a nonsense, a frameshift, and 3 splice site mutations. Five mutations were confirmed as de novo events. One mutation was cosegregated with familial porencephaly, and 2

View this article online at wileyonlinelibrary.com. DOI: 10.1002/ana.23736

Received Jun 8, 2012, and in revised form Aug 6, 2012. Accepted for publication Aug 10, 2012.

Address correspondence to Dr Saitsu, Department of Human Genetics, Yokohama City University Graduate School of Medicine, 3-9 Fukuura, Kanazawa-ku, Yokohama 236-0004, Japan. E-mail: hsaitsu@yokohama-cu.ac.jp

From the [1]Department of Human Genetics, Yokohama City University Graduate School of Medicine, Yokohama; [2]Department of Pediatrics, Tohoku University School of Medicine, Sendai; [3]Department of Pediatric Neurology, Takuto Rehabilitation Center for Children, Sendai; [4]Department of Pediatrics, Yamagata University Faculty of Medicine, Yamagata; [5]Division of Neurology, Clinical Research Institute, Kanagawa Children's Medical Center, Yokohama; [6]Department of Pediatric Neurology, Seirei-Mikatahara General Hospital, Hamamatsu; [7]Department of Pediatric Neurology, Morinomiya Hospital, Osaka; [8]Department of Pathology, Brain Research Institute, University of Niigata, Niigata; [9]Comprehensive Epilepsy Center; [10]Department of Pathology, Seirei Hamamatsu General Hospital, Shizuoka; [11]Department of Pediatrics, Toyohashi Municipal Hospital, Toyohashi; [12]Division of Child Neurology, Tottori University Faculty of Medicine, Yonago; [13]Division of Child Neurology, Department of Brain and Neurosciences, Tottori University Faculty of Medicine, Yonago; [14]Department of Pediatrics, Asahikawa Medical University, Asahikawa; [15]Department of Neurology, Nagano Children's Hospital, Azumino; [16]Department of Pediatrics, Kameda Medical Center, Chiba; [17]Department of Pediatrics, Juntendo University Faculty of Medicine, Tokyo; [18]Aichi Welfare Center for Persons with Developmental Disabilities, Kasugai; [19]Department of Pediatrics, Yodogawa Christian Hospital, Osaka; [20]Department of Pediatrics and Neonatology, Nagoya City University Graduate School of Medical Sciences, Nagoya; [21]Department of Pediatric Neurosurgery, Takatsuki General Hospital, Osaka; and [22]Department of Pediatrics, Kitano Hospital, Tazuke Kofukai Medical Research Institute, Osaka, Japan.

Additional supporting information can be found in the online version of this article.

mutations were inherited from asymptomatic parents. Aberrant splicing was demonstrated by reverse transcriptase polymerase chain reaction analyses in 2 patients with splice site mutations.
Interpretation: Our study first confirmed that *COL4A1* mutations are associated with schizencephaly and hemolytic anemia. Based on the finding that *COL4A1* mutations were frequent in patients with porencephaly and schizencephaly, genetic testing for *COL4A1* should be considered for children with these conditions.

ANN NEUROL 2013;73:48–57

Type IV collagens are basement membrane proteins that are expressed in all tissues, including the vasculature. COL4A1 (α1 chain) and COL4A2 (α2 chain) are the most abundant type IV collagens, and form heterotrimers with a 2:1 stoichiometry (α1α1α2).[1] Mutations in *COL4A1* and *COL4A2* cause sporadic and hereditary porencephaly, a neurological disorder characterized by fluid-filled cysts in the brain that often cause hemiplegia or tetraplegia.[2–4] In addition, a variety of clinical phenotypes, including small vessel disease affecting the brain, eyes, and kidneys, are associated with *COL4A1* abnormality[5,6]: neonatal porencephaly and adult stroke,[7] sporadic extensive bilateral porencephaly resembling hydranencephaly,[8] periventricular leukomalacia with intracranial calcification,[9] HANAC (hereditary angiopathy with nephropathy, aneurysm, and muscle cramps) syndrome,[10,11] Axenfeld–Rieger anomaly with leukoencephalopathy, and adult stroke and intracerebral hemorrhage.[12–14] Notably, *COL4A1* mutations were present in 2 patients with muscle–eye–brain/Walker–Warburg syndrome (MEB/WWS), which is characterized by ocular dysgenesis, neuronal migration defects, and congenital muscular dystrophy, suggesting that *COL4A1* is also involved in normal cortical and muscular development in humans.[15] Consistent with this hypothesis, a mouse model of a heterozygous *COL4A1* mutation (*Col4a1*$^{+/\Delta ex40}$) showed ocular dysgenesis, cortical neuronal localization defects, and myopathy, along with cerebral hemorrhage and porencephaly.[2,15] The phenotypic spectrum of *COL4A1* mutations is expanding; however, the whole spectrum of systemic phenotypes and the incidence of *COL4A1* mutations associated with porencephaly has not been systemically examined.

In this study, we screened for *COL4A1* mutations in 61 patients with porencephaly and 10 patients with schizencephaly, which may be similarly caused by disturbed vascular supply leading to cerebral degeneration, but can be distinguished depending on time of insult.[2–4,16,17] *COL4A1* mutations were identified in 10 patients with porencephaly and 5 patients with schizencephaly, who showed a variety of associated findings, including intracranial calcification, focal cortical dysplasia (FCD), ocular abnormalities, pontocerebellar atrophy, myopathy, elevated serum creatine kinase levels, and hemolytic anemia. Our study demonstrated the importance of genetic testing for *COL4A1* in children with porencephaly or schizencephaly.

Patients and Methods

Patients

A total of 61 patients with porencephaly including a previous cohort with porencephaly,[4] and 10 patients with schizencephaly including a patient who also had porencephaly were analyzed for *COL4A1* mutations. Schizencephaly is defined as transmantle clefts bordered by polymicrogyria in adjacent cortex.[18] The clefts extended through the entire hemisphere, from the ependymal lining of the lateral ventricles to the pial covering of the cortex.[19] The clefts are further divided into those with closed lips and those with open lips. In the clefts with closed lips, the walls affix each other directly, obliterating the cerebrospinal fluid space within the cleft at that point.[20] *COL4A2* mutations were negative for these patients. Genomic DNA was isolated from blood leukocytes according to standard methods, and amplified using an illustra GenomiPhi V2 DNA Amplification Kit (GE Healthcare, Buckinghamshire, UK). The DNA of familial members of patient 6 was isolated from saliva samples using Oragene (DNA Genotek, Kanata, Ontario, Canada). Experimental protocols were approved by the committee for ethical issues at Yokohama City University School of Medicine. All patients were investigated in agreement with the requirements of Japanese regulations.

Mutation Analysis

Exons 1 to 52, covering the entire *COL4A1* coding region, were examined by high-resolution melting (HRM) curve analysis. Samples showing an aberrant melting curve pattern in the HRM analysis were sequenced. Polymerase chain reaction (PCR) primers and conditions are shown in Supplementary Table S1. All novel mutations were verified using original genomic DNA, and screened in 200 Japanese normal controls by HRM analysis. For the family showing de novo mutations, parentage was confirmed by microsatellite analysis, as previously described.[21] Biological parents were confirmed if >4 informative markers were compatible and other markers showed no discrepancy.

Reverse Transcriptase-PCR

Reverse transcriptase (RT)-PCR using total RNA extracted from lymphoblastoid cell lines (LCL) was performed essentially as previously described.[22] Briefly, total RNA was extracted using RNeasy Plus MiniKit (Qiagen, Tokyo, Japan) from LCL with or without 30μM cycloheximide (CHX; Sigma, Tokyo, Japan) incubation for 4 hours. Four micrograms total RNA was subjected to reverse transcription, and 2μl cDNA was used for PCR. Primer sequences are ex20-F (5′-CCCAAAAGGTTTCC CAGGACTACCA-3′) and ex22-R (5′-GTCCGGGCTGACAT TCCACAATTC-3′; for patient 4); and ex22-F (5′-GAATTC-CAGGGCAGCCAGGATTTAT-3′) and ex24-R (5′-CATCTCT GCCAGGCAAACCTCTGT-3′; for patient 7). DNA of each

PCR band was purified by QIAEXII Gel extraction kit (Qiagen; for patient 4) and E.Z.N.A. poly-Gel DNA Extraction kit (Omega Bio-Tek, Norcross, GA; for patient 7), respectively.

Results

Mutation and RT-PCR analysis

COL4A1 abnormalities were identified in 15 patients (Fig 1 and Table). Nine mutations occurred at highly conserved Gly residues in the Gly-X-Y repeat of the collagen triple helical domain. Interestingly, a missense mutation (c.4843G>A [p.Glu1615Lys]) at an evolutionary conserved amino acid and a nonsense mutation (c.4887C>A [p.Tyr1629X]) were found in the carboxy-terminal noncollagenous (NC1) domain. The other 4 mutations include a frameshift mutation (c.2931dupT [p.Gly978TrpfsX15]) and 3 splice site mutations (c.1121-2dupA, c.1382-1G>C, and c.1990+1G>A). None of these mutations was present in 200 Japanese normal controls, and Web-based prediction tools suggested that these mutations are pathogenic (Supplementary Table S2). The c.2842G>A (patient 1), c.3976G>A (patient 2), c.4887C>A (patient 8), c.2689G>A (patient 13), and c.1990+1G>A (patient 14) mutations occurred de novo. The c.3995G>A mutation (patient 3) was not found in the mother's DNA (the father's DNA was unavailable). The c.1121-2dupA (patient 4) and c.2931dupT (patient 6) mutations were found in the asymptomatic fathers. c.1963G>A (patient 10) was found in familial members affected with porencephaly as well as asymptomatic carriers, suggesting incomplete penetrance of the mutation (Supplementary Fig S1). The remaining patients' parental DNA was unavailable.

To examine the mutational effects of the 2 splice acceptor site mutations (c.1121-2dupA and c.1382-1G>C), RT-PCR and sequencing were performed (see Fig 1). c.1121-2dupA caused the deletion of exon 21 from the wild-type *COL4A1* mRNA, resulting in an in-frame 55-amino acid deletion (p.Gly374_Asn429delinsAsp). The effect of c.1382-1G>C was more complicated. There were 3 PCR products amplified from LCL treated with CHX, which inhibits nonsense-mediated mRNA decay (NMD). The middle band corresponded to the wild-type allele. The sequence of the lower mutant band showed a 33bp insertion of intron 22 and an 84bp deletion of all of exon 23 from the use of cryptic splice acceptor and donor sites within intron 22. The change of amino acid sequence from this mutant transcript was a deletion of 29 amino acids and an insertion of 12 amino acids (p.Gly461_Gly489delinsValHisCysGlyAspPheTrpSerHisValThrArg). The upper band was only observed in CHX-treated LCL, but was not evident in the untreated LCL, suggesting that this mutant transcript may undergo NMD. Sequencing of the upper band showed a 61bp insertion of intron 22 from the use of a cryptic splice acceptor site within intron 22, as mentioned above. The product of this mutant transcript leads to a frameshift, creating a premature stop codon (p.Gly461ValfsX31), which is consistent with degradation of the mutant transcript by NMD.

Clinical Features

The clinical information for individuals with *COL4A1* mutations is summarized in the Table, and their representative brain images are shown in Figure 2 and Supplementary Fig S2. *COL4A1* mutations were identified in 10 of 61 patients with porencephaly (16.4%). Of note, *COL4A1* mutations were identified in 5 of 10 patients with schizencephaly (50.0%), revealing a novel association between *COL4A1* mutations and schizencephaly. Thirteen patients were born at term, and 2 patients (patients 1 and 12) were born at preterm. Their body weight was normal at birth except for 5 patients (patients 3, 4, 9, 12, and 15) who were below −2.0 standard deviations. The occipitofrontal circumference was available in 12 patients, and 6 patients (patients 2, 3, 6, 13, 14, and 15) were below −2.0 standard deviations. Two patients (patients 11 and 12) were confirmed to have an antenatal hemorrhage as previously reported.[23,24] Among associated findings with *COL4A1* mutations, a patient showed FCD that was histologically demonstrated (Fig 3A–F). In addition, hemolytic anemia was found in 5 of 15 patients, suggesting that hemolytic anemia may be a novel feature associated with *COL4A1* mutation. Pontocerebellar atrophy along with severe bilateral porencephaly was observed in 2 patients, and a patient showed cerebellar hypoplasia. Previously reported magnetic resonance imaging and systemic findings associated with *COL4A1* mutations were also observed, including intracranial calcification (7 of 15), myopathy (1 of 15; see Fig 3G, H), ocular abnormalities (4 of 15), and elevated serum creatine kinase levels (6 of 15), confirming that these features are useful signs for *COL4A1* testing. Case reports are available in the Supplementary Data.

Discussion

We found a total of 15 novel mutations in this study. Nine mutations occurred at highly conserved Gly residues in the Gly-X-Y repeat of the collagen triple helical domain, suggesting that these mutations may alter the collagen IV $\alpha1\alpha1\alpha2$ heterotrimers.[1,25] We reported for the first time 2 mutations (a nonsense and a missense change) in the NC1 domain. The nonsense mutation

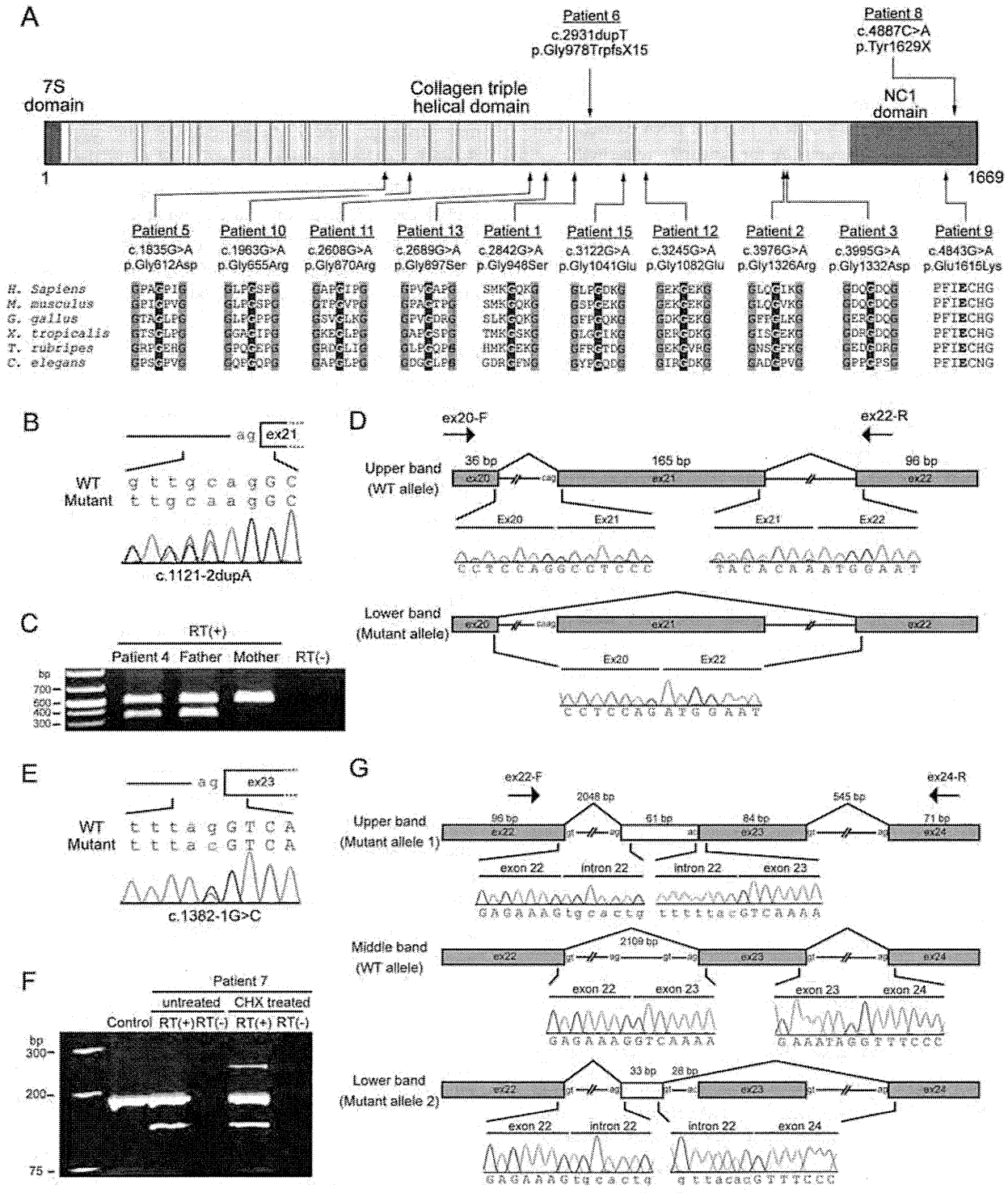

FIGURE 1: *COL4A1* mutations in patients with porencephaly or schizencephaly. (A) Functional domains of COL4A1 protein. The locations of 12 mutations, including 10 missense mutations (bottom), a nonsense mutation, and a frameshift mutation (top) are indicated by arrows. The 7S domain is highlighted with blue and the NC1 domain with red. Gly-X-Y repeats within the collagen triple helical domain are highlighted with yellow. All of the missense mutations occurred at evolutionary conserved amino acids. The positions of the conserved Gly residues in the Gly-X-Y repeats are highlighted in gray. Homologous sequences were aligned using CLUSTALW (http://www.genome.jp/tools/clustalw/). (B) The c.1121-2dupA mutation in intron 20 is colored red. Sequences of exons and introns are presented in upper and lower cases, respectively. (C) Reverse transcriptase (RT)-polymerase chain reaction (PCR) analysis of patient 4 and his parents. (D) Schematic presentation of the wild-type (WT; upper) and mutant (lower) transcripts and primers used for analysis. A single band (500bp), corresponding to the WT allele, was amplified using the mother's cDNA template. Conversely, a lower band was detected from the cDNA from the patient and his father. In the mutant transcript, the 165bp exon 21 was deleted. Sequences of exons and introns are presented in upper and lower cases, respectively. (E) The c.1382-1G>C mutation in intron 22 is colored red. (F) RT-PCR analysis of patient 7 and a control. (G) Schematic representation of the WT and mutant transcripts, and primers used for analysis. A single band (183bp), corresponding to the WT allele, was amplified using a control cDNA template. Conversely, upper and lower bands were detected from the patient's cDNA. The upper band (244bp), which was observed only in cycloheximide (CHX)-treated cells, had a 61bp insertion of intron 22 sequences, leading to a frameshift. Absence of the upper band in untreated lymphoblastoid cell lines strongly suggests that the mutant transcript may undergo nonsense-mediated mRNA decay. The lower band had a 33bp insertion of intron 22 and 84bp deletion of the whole of exon 23, leading to an in-frame 51bp deletion.

TABLE: Clinical features of patients with *COL4A1* mutations

Cases	Age	Sex	Mutation	Inheritance	Brain MRI/ CT findings	CP	Epi	Ocular features	Family history	ID	Hyper-CK	Other
1	14y	M	c.2842G>A (p.Gly948Ser)	de novo	Bilateral POCE, calcification, hemosiderin deposition	Q	+	-	-	+	-	
2	18m	M	c.3976G>A (p.Gly1326Arg)	de novo	Bilateral SCZ, calcification, hemosiderin deposition	Q	+	-	-	+	-	
3	15m	M	c.3995G>A (p.Gly1332Asp)	Absent in mother	Unilateral SCZ, calcification, hemosiderin deposition	H	+	-	-	+	-	
4	6y	M	c.1121-2dupA[1)]	Paternal	Unilateral POCE	H	+	-	-	+	-	FCD
5	2m	F	c.1835G>A (p.Gly612Asp)	ND	Bilateral SCZ, calcification, thin CC, thin brain stem, cerebellar atrophy, absence of SP, hemosiderin deposition, multicystic encephalomalacia,	Q	+	Optic nerve hypoplasia	-	+	+	HA
6	7y	M	c.2931dupT (p.Gly978TrpfsX15)	Paternal	Unilateral POCE	H	+	-	-	+	+	
7	12y	F	c.1382-1G>C[2)]	ND	Unilateral POCE	H	+	-	-	+	+	Myopathy
8	10y	M	c.4887C>A (p.Tyr1629X)	de novo	Unilateral POCE	H	+	-	Hematuria	+	-	
9	3m	F	c.4843G>A (p.Glu1615Lys)	ND	Bilateral POCE, calcification, hypoplastic CC, hemosiderin deposition, thin	Q	+	Microphthalmia Corneal opacity	-	+	-	VSD, HA

TABLE (Continued)

Cases	Age	Sex	Mutation	Inheritance	Brain MRI/ CT findings	CP	Epi	Ocular features	Family history	ID	Hyper-CK	Other
					brain stem, cerebellar atrophy, multicystic encephalomalacia							
10	2y7m	F	c.1963G>A (p.Gly655Arg)	Paternal[3)]	Bilateral POCE	Q	+	-	POCE, Epi	+	-	-
11	1y	F	c.2608G>A (p.Gly870Arg)	ND	Unilateral POCE, calcification	Q	+	Congenital cataract	-	+	-	-
12	1y5m	M	c.3245G>A (p.Gly1082Glu)	ND	Unilateral SCZ with bilateral POCE, calcification, cerebellar hypoplasia	T	+	Congenital cataract	-	+	-	HA, Hematuria
13	3y7m	M	c.2689G>A (p.Gly897Ser)	de novo	Unilateral POCE	Q	+	-	-	+	+	-
14	9m	F	c.1990+1G>A	de novo	Unilateral POCE, hemosiderin deposition	Q	+	-	-	+	+	HA, Hematuria
15	2y	F	c.3122G>A (p.Gly1041Glu)	ND	Unilateral SCZ, hemosiderin deposition	Q	+	-	-	+	+	HA

1) p.Gly374_Asn429delinsAsp change was predicted by mRNA analysis
2) Two alternative protein chages were predicted by mRNA analysis: p.Gly461_Gly489delinsValHisCysGlyAspPheTrpSerHisValThrArg and p.Gly461ValfsX31. y, years; m, months; M, male; F, female; ND, Not determined; POCE, porencephaly, SCZ, schizencephaly; CC, corpus callosum; SP, septum pellucidum; CP, cerebral palsy; H, hemiplegia; T, Triplegia; Q, quadriplegia; Epi, epilepsy; ID, intellectual disability; CK, creatine kinase; FCD, Focal cortical dysplasia; HA, Hemolytic anemia; VSD, ventricular septal defect
3) Co-segregation of the p.Gly655Arg mutation with porencephaly was confirmed.

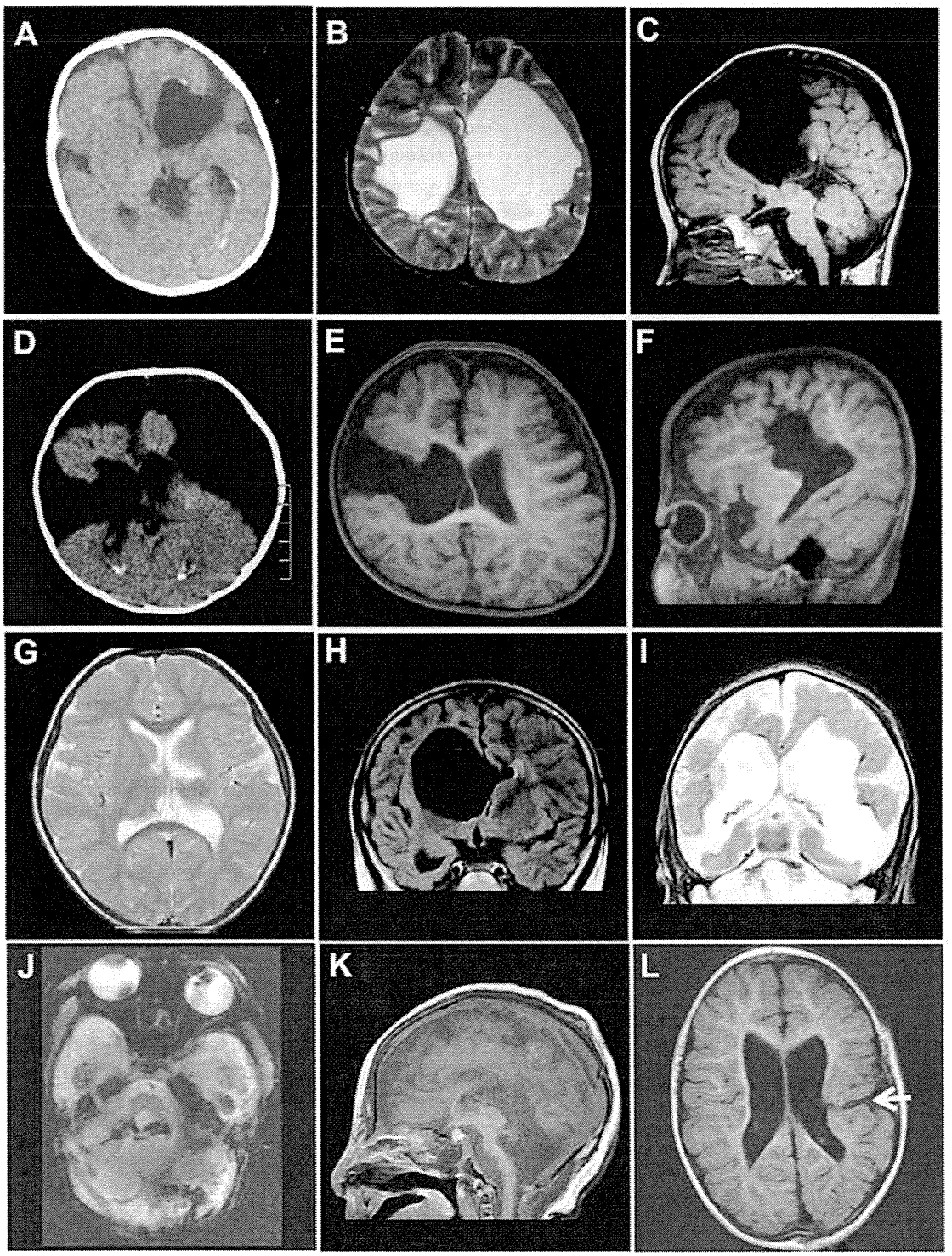

FIGURE 2: Computed tomography (CT) scan (A, D) and magnetic resonance imaging (MRI; B, C, E–L) of patients with *COL4A1* mutations. (A–C) Images of patient 1. (A) The CT scan shows calcification along with the dilated lateral ventricular wall. (B) T2-weighted and (C) T1-weighted images (WIs) at 5 years of age showing bilateral porencephaly. (D) The CT image of patient 2 with schizencephaly shows calcification of the lateral ventricular wall and brain parenchyma. (E, F) T1-WIs of patient 3 show unilateral schizencephaly at 15 months of age. (G) T2-WI of patient 4 at 3 years of age shows parenchymal defect of the left thalamus and basal ganglia due to subependymal hemorrhage. (H) Fluid-attenuated inversion recovery image of patient 7 at 6 years of age showing unilateral porencephaly. (I) T2-WI, (J) T2*-weighted gradient-echo image (WGRE), and (K) T1-WI of patient 9. (I) The MRI at 2 months of age shows bilateral porencephaly with low-intensity lesions along with a deformed ventricular wall, which has hemosiderin deposition and calcification. (J) T2*-WGRE showing hemosiderin deposition in the atrophic cerebellum. The atrophic pontocerebellar structures are also shown in (K). (L) T1-WI of patient 15 showed schizencephaly in the left hemisphere at 2 years of age.

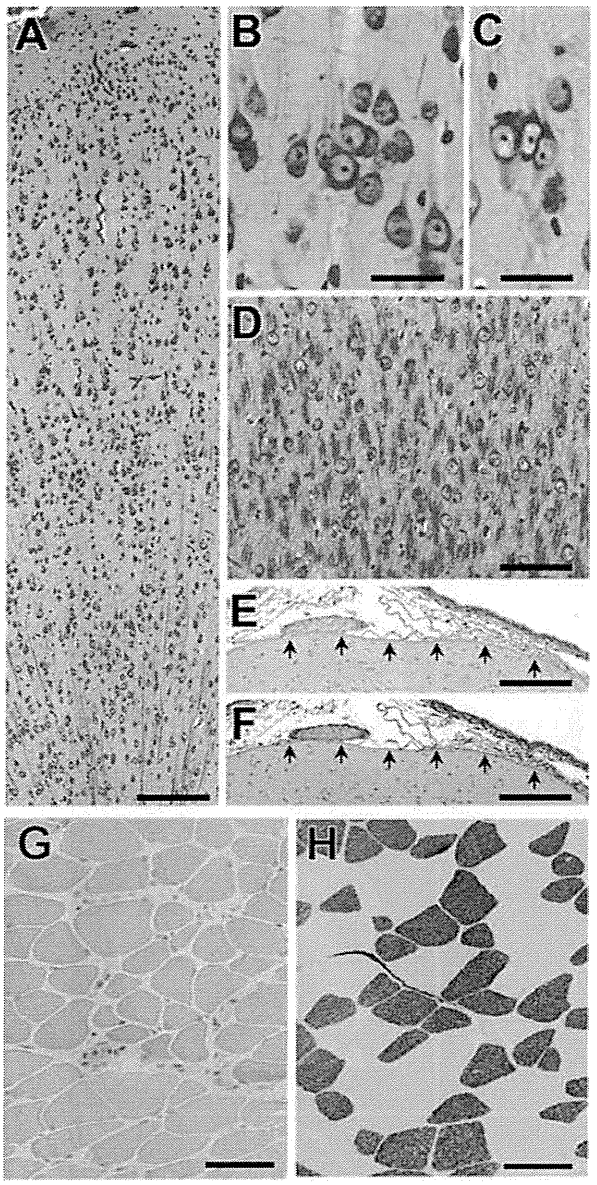

FIGURE 3: Histopathological features of the resected frontal tissue of patient 4 (A–F) and biopsied rectus abdominis muscle of patient 7 (G, H). (A) Low-magnification view of the cortex showing architectural abnormalities. (B, C) Two examples of neuronal clustering. (D) Many neurons scattered within the subcortical white matter. (E, F) Two serial sections demonstrating the superficial layer of the cortex. Note that the basal lamina of the pia mater (*arrows* in each panel) is continuously labeled with antibodies against collagen type IV (E) and laminin (F). (A–D) Klüver–Barrera stain. (E, F) Immunostained and then counterstained with hematoxylin. (G) Hematoxylin and eosin staining showing variation in fiber size, slightly increased endomysial connective tissue, and internal nuclei. (H) Adenosine triphosphatase (pH 4.5) staining showing type 2B fiber deficiency. There was no increase in number of type 2C fibers. Scale bars indicate 175μm (A, E, F), 30μm (B, C), 80μm (D), and 30μm (G, H).

would cause a truncation of the NC1 domain rather than mRNA degradation by NMD as the mutation was located within 50bp of the exon–intron boundary of the second to last exon (exon 51).[26] The NC1 domains are the sites for molecular recognition through which the stoichiometry of chains in the assembly of triple-helical formation is directed[1]; therefore, these 2 mutations may alter the assembly of the collagen IV $\alpha1\alpha1\alpha2$ heterotrimers. In addition, the effect of 2 splice site mutations was examined using LCL, suggesting that in-frame deletion/insertion mutant protein should be produced. Thus, it is highly likely that impairment of the collagen IV $\alpha1\alpha1\alpha2$ heterotrimer assembly caused by mutant $\alpha1$ chain is a common pathological mechanism of *COL4A1* mutations. The c.2931dupT mutation found in patient 6 and his father might cause severe truncation of COL4A1 protein. It is possible that the truncation of COL4A1 protein can also impair $\alpha1\alpha1\alpha2$ heterotrimer assembly similar to substitutions of conserved Gly residues in the Gly-X-Y repeat. Alternatively, the mutant transcript might undergo NMD, and haploinsufficiency of *COL4A1* might cause a weakness of basement membrane. Biological analysis using patients' cells will clarify these possibilities.

COL4A1 mutations in schizencephaly were first demonstrated in this study. Schizencephaly was used by Yakovlev and Wadsworth in 1946 to describe true clefts formed in the brain as a result of failure of development of the cortical mantle in the zones of cleavage of the primary cerebral fissures.[19] Schizencephaly is differentiated from clefts in the central mantle that arise as the result of a destruction of the cerebral tissues, which they called encephalocrastic porencephalies, now known simply as porencephaly.[19] Schizencephaly has been understood as a neuronal migration disorder, because the clefts are lined by abnormal gray matter, described as polymicrogyria. Conversely, porencephaly is understood to be a postmigration accident resulting in lesions, without gray matter lining the clefts or an associated malformation of cortical development. It has been suggested that both schizencephaly and porencephaly are caused by encephaloclastic regions, and can be distinguished depending on time of insult.[16,17] The present study clearly demonstrated that *COL4A1* mutations caused both porencephaly and schizencephaly, supporting the same pathological mechanism for these 2 conditions.

The genes responsible for FCD have been elusive, despite extensive investigation. The pathological features of the cortical tubers of tuberous sclerosis (TSC) may be indistinguishable from those of FCD. Apart from FCD due to TSC, there is only 1 gene that may explain the genetic basis of FCD, where a homozygous mutation in *CNTNAP2* has been identified in Amish children with FCD, macrocephaly, and intractable seizures.[27] Surprisingly, the present study discovered a patient with FCD

and porencephaly, in whom aberrant splicing was demonstrated and FCD1A was pathologically confirmed using resected brain tissues. A recent report revealed *COL4A1* mutations in 2 patients with MEB/WWS showing cobblestone lissencephaly,[15] and abnormal cortical development has been observed in mouse models of *COL4A1* mutations.[15,28] Thus, it is possible that *COL4A1* mutations are involved in cerebral cortical malformations, including FCD. Identification of a greater number of cases is required to confirm the association between *COL4A1* mutations and cortical malformations in humans.

In a few children, the sequelae were much more severe than would be expected on the basis of their imaging findings. This is of importance when counseling parents with regard to prediction of neurodevelopmental outcome.

Two patients with *COL4A1* mutations showed intracranial calcification, pontocerebellar atrophy, ocular abnormalities, and hemolytic anemia associated with severe bilateral porencephaly (patient 9) or schizencephaly (patient 5). Severe hemorrhagic destructive lesions in the cerebrum were observed in these patients, and T2* images also showed hemorrhage in the cerebellum, which may have resulted in a thin brainstem and severe cerebellar atrophy. Thus, these 2 patients could be considered as the most severe manifestations affecting the developing brain and eyes. A common feature of the 2 patients is hemolytic anemia of an unknown cause, which required frequent blood transfusions. Five of 15 patients with *COL4A1* mutations showed hemolytic anemia. Interestingly, 2 reports have demonstrated that mouse *Col4a1* mutants showed a significant reduction in red blood cell (RBC) number and hematocrit.[28,29] Given that *Col4a1* mutations lead to hemorrhage, chronic hemorrhage is possibly involved in RBC loss. Alternatively, the *Col4a1* mutation may directly affect blood progenitor cells, as they transmigrate across basement membranes before entering the peripheral blood.[30] Hemolytic anemia in patients with *COL4A1* mutations would imply the latter explanation. Further studies are required to clarify how *COL4A1/Col4a1* mutations are involved in anemia.

In summary, we found 15 mutations in *COL4A1* among 71 patients with porencephaly or schizencephaly, showing an unexpectedly high percentage of mutations (about 21%) in these patients. Fourteen patients with *COL4A1* mutations had no family history of cerebral palsy. The 15 patients with *COL4A1* mutations showed a variety of phenotypes, further expanding the possible clinical spectrum of *COL4A1* mutations to include schizencephaly, FCD, pontocerebellar atrophy, and hemolytic anemia. Genetic testing for *COL4A1* should be recommended for children with porencephaly and schizencephaly.

Acknowledgment

This work was supported by research grants from the Ministry of Health, Labor, and Welfare (K.H., M.K., H.O., N.Mi., N.Ma., H.S.), Japan Science and Technology Agency (N.Ma.), and Strategic Research Program for Brain Sciences (11105137 to N.Ma.), a Grant-in-Aid for Scientific Research on Innovative Areas (Foundation of Synapse and Neurocircuit Pathology) from the Ministry of Education, Culture, Sports, Science, and Technology of Japan (11001956 to N.Ma.), a Grant-in-Aid for Scientific Research from the Japan Society for the Promotion of Science (H.O., N.Ma.), a Grant-in-Aid for Young Scientists from the Japan Society for the Promotion of Science (H.D., N.Mi., H.S.), and a grant from the Takeda Science Foundation (N.Mi., N.Ma.). This work was performed at the Advanced Medical Research Center, Yokohama City University, Japan.

We thank the patients and their family members for their participation in this study.

Authorship

Y.Y. and K.H. contributed equally to this work.

Potential Conflicts of Interest

Nothing to report.

References

1. Khoshnoodi J, Pedchenko V, Hudson BG. Mammalian collagen IV. Microsc Res Tech 2008;71:357–370.
2. Gould DB, Phalan FC, Breedveld GJ, et al. Mutations in Col4a1 cause perinatal cerebral hemorrhage and porencephaly. Science 2005;308:1167–1171.
3. Breedveld G, de Coo IF, Lequin MH, et al. Novel mutations in three families confirm a major role of COL4A1 in hereditary porencephaly. J Med Genet 2006;43:490–495.
4. Yoneda Y, Haginoya K, Arai H, et al. De novo and inherited mutations in COL4A2, encoding the type IV collagen alpha2 chain cause porencephaly. Am J Hum Genet 2012;90:86–90.
5. Vahedi K, Alamowitch S. Clinical spectrum of type IV collagen (COL4A1) mutations: a novel genetic multisystem disease. Curr Opin Neurol 2011;24:63–68.
6. Lanfranconi S, Markus HS. COL4A1 mutations as a monogenic cause of cerebral small vessel disease: a systematic review. Stroke 2010;41:e513–e518.
7. van der Knaap MS, Smit LM, Barkhof F, et al. Neonatal porencephaly and adult stroke related to mutations in collagen IV A1. Ann Neurol 2006;59:504–511.
8. Meuwissen ME, de Vries LS, Verbeek HA, et al. Sporadic COL4A1 mutations with extensive prenatal porencephaly resembling hydranencephaly. Neurology 2011;76:844–846.

9. Livingston J, Doherty D, Orcesi S, et al. COL4A1 Mutations associated with a characteristic pattern of intracranial calcification. Neuropediatrics 2011;42:227–233.
10. Plaisier E, Gribouval O, Alamowitch S, et al. COL4A1 mutations and hereditary angiopathy, nephropathy, aneurysms, and muscle cramps. N Engl J Med 2007;357:2687–2695.
11. Alamowitch S, Plaisier E, Favrole P, et al. Cerebrovascular disease related to COL4A1 mutations in HANAC syndrome. Neurology 2009;73:1873–1882.
12. Coutts SB, Matysiak-Scholze U, Kohlhase J, Innes AM. Intracerebral hemorrhage in a young man. CMAJ 2011;183:E61–E64.
13. Sibon I, Coupry I, Menegon P, et al. COL4A1 mutation in Axenfeld-Rieger anomaly with leukoencephalopathy and stroke. Ann Neurol 2007;62:177–184.
14. Weng YC, Sonni A, Labelle-Dumais C, et al. COL4A1 mutations in patients with sporadic late-onset intracerebral hemorrhage. Ann Neurol 2012;71:470–477.
15. Labelle-Dumais C, Dilworth DJ, Harrington EP, et al. COL4A1 mutations cause ocular dysgenesis, neuronal localization defects, and myopathy in mice and Walker-Warburg syndrome in humans. PLoS Genet 2011;7:e1002062.
16. Friede R. Porencephaly, hydranencephaly, multicystic encephalopathy. In: Developmental neuropathology. 2nd ed. Berlin, Germany: Springer-Verlag, 1989:28–43.
17. Govaert P. Prenatal stroke. Semin Fetal Neonatal Med 2009;14: 250–266.
18. Barkovich AJ, Guerrini R, Kuzniecky RI, et al. A developmental and genetic classification for malformations of cortical development: update 2012. Brain 2012;135:1348–1369.
19. Yakovlev PI, Wadsworth RC. Schizencephalies; a study of the congenital clefts in the cerebral mantle; clefts with fused lips. J Neuropathol Exp Neurol 1946;5:116–130.
20. Barkovich AJ, Kjos BO. Schizencephaly: correlation of clinical findings with MR characteristics. AJNR Am J Neuroradiol 1992;13: 85–94.
21. Saitsu H, Kato M, Mizuguchi T, et al. De novo mutations in the gene encoding STXBP1 (MUNC18–1) cause early infantile epileptic encephalopathy. Nat Genet 2008;40:782–788.
22. Saitsu H, Kato M, Okada I, et al. STXBP1 mutations in early infantile epileptic encephalopathy with suppression-burst pattern. Epilepsia 2010;51:2397–2405.
23. Lichtenbelt KD, Pistorius LR, De Tollenaer SM, et al. Prenatal genetic confirmation of a COL4A1 mutation presenting with sonographic fetal intracranial hemorrhage. Ultrasound Obstet Gynecol 2012;39:726–727.
24. de Vries LS, Koopman C, Groenendaal F, et al. COL4A1 mutation in two preterm siblings with antenatal onset of parenchymal hemorrhage. Ann Neurol 2009;65:12–18.
25. Engel J, Prockop DJ. The zipper-like folding of collagen triple helices and the effects of mutations that disrupt the zipper. Annu Rev Biophys Biophys Chem 1991;20:137–152.
26. Nagy E, Maquat LE. A rule for termination-codon position within intron-containing genes: when nonsense affects RNA abundance. Trends Biochem Sci 1998;23:198–199.
27. Strauss KA, Puffenberger EG, Huentelman MJ, et al. Recessive symptomatic focal epilepsy and mutant contactin-associated protein-like 2. N Engl J Med 2006;354:1370–1377.
28. Favor J, Gloeckner CJ, Janik D, et al. Type IV procollagen missense mutations associated with defects of the eye, vascular stability, the brain, kidney function and embryonic or postnatal viability in the mouse, Mus musculus: an extension of the Col4a1 allelic series and the identification of the first two Col4a2 mutant alleles. Genetics 2007;175:725–736.
29. Van Agtmael T, Bailey MA, Schlotzer-Schrehardt U, et al. Col4a1 mutation in mice causes defects in vascular function and low blood pressure associated with reduced red blood cell volume. Hum Mol Genet 2010;19:1119–1128.
30. Janowska-Wieczorek A, Marquez LA, Nabholtz JM, et al. Growth factors and cytokines upregulate gelatinase expression in bone marrow CD34(+) cells and their transmigration through reconstituted basement membrane. Blood 1999;93:3379–3390

SCIENTIFIC REPORTS

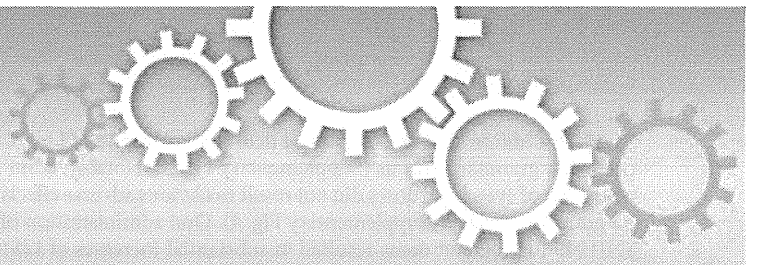

SUBJECT AREAS:
DRUG DISCOVERY AND DEVELOPMENT
NEURODEVELOPMENTAL DISORDERS
DEVELOPMENTAL DISORDERS
MOLECULAR NEUROSCIENCE

Received
11 October 2012

Accepted
15 January 2013

Published
6 February 2013

Correspondence and requests for materials should be addressed to S.H. (shinjih@med.osaka-cu.ac.jp)

* These authors contributed equally to this work.

Post-natal treatment by a blood-brain-barrier permeable calpain inhibitor, SNJ1945 rescued defective function in lissencephaly

Shiori Toba[1]*, Yasuhisa Tamura[2]*, Kanako Kumamoto[1]*, Masami Yamada[1], Keizo Takao[3,4], Satoko Hattori[3,5], Tsuyoshi Miyakawa[3,4,5], Yosky Kataoka[2], Mitsuyoshi Azuma[6], Kiyoshi Hayasaka[7], Masano Amamoto[8], Keiko Tominaga[9], Anthony Wynshaw-Boris[10], Hideki Wanibuchi[11], Yuichiro Oka[12,13,14], Makoto Sato[12,13,14], Mitsuhiro Kato[7] & Shinji Hirotsune[1]

[1]Department of Genetic Disease Research, Osaka City University Graduate School of Medicine, Asahi-machi 1-4-3 Abeno, Osaka 545-8586, Japan, [2]Cellular Function Imaging Laboratory, RIKEN Center for Molecular Imaging Science, Minatojima minamimachi, Chuo-ku, Kobe, Hyogo, Japan, [3]Japan Science and Technology Agency, CREST, 4-1-8 Honcho, Kawaguchi, Saitama 332-0012, Japan, [4]Section of Behavior Patterns, Center for Genetic Analysis of Behavior National Institute for Physiological Sciences, 38 Nishigonaka Myodaiji, Okazaki, Aichi, 444-8585, Japan, [5]Division of Systems Medical Science, Institute for Comprehensive Medical Science, Fujita Health University, Toyoake, Aichi 470-1192, Japan, [6]Senju Laboratory of Ocular Sciences, Senju Pharmaceutical Co., Ltd., 1-5-4, Murotani, Nishi-ku, Kobe, Hyogo 651-2241, Japan, [7]Department of Pediatrics, Yamagata University Faculty of Medicine, Iida-nishi 2-2-2, Yamagata 990-9585, Japan, [8]Pediatric Emergency Center, Kitakyuusyu City Yahata Hospital. Nishimotomachi 4-18-1, Yahatahigasi Kitakyuusyu City, Japan, [9]Department of Internal Medicine, Tokyo Metropolitan Fuchu Medical Center for the Disabled. Musashidai, Fuchu-shi, Tokyo, Japan, [10]Department of Pediatrics and Institute for Human Genetics, University of California, San Francisco, School of Medicine, San Francisco, CA 94143-0794, [11]Department of Pathology, Osaka City University Graduate School of Medicine, Asahi-machi 1-4-3 Abeno, Osaka 545-8586, Japan, [12]Division of Cell Biology and Neuroscience, Department of Morphological and Physiological Sciences, Faculty of Medical Sciences, University of Fukui, [13]Research Center for Child Mental Development, University of Fukui, [14]Research and Education Program for Life Science, University of Fukui.

Toward a therapeutic intervention of lissencephaly, we applied a novel calpain inhibitor, SNJ1945. Peri-natal or post-natal treatment with SNJ1945 rescued defective neuronal migration in *Lis1*$^{+/-}$ mice, impaired behavioral performance and improvement of ^{18}F-FDG uptake. Furthermore, SNJ1945 improved the neural circuit formation and retrograde transport of NFG in *Lis1*$^{+/-}$ mice. Thus, SNJ1945 is a potential drug for the treatment of human lissencephaly patients.

LIS1 encodes a protein carrying seven WD repeats[1,2] that was first identified as a non-catalytic subunit of platelet activating factor-acetylhydrolase (Pafah1b1)[3]. Numerous studies to address the molecular function of LIS1 led to the conclusion that LIS1 is essential for the proper regulation of cytoplasmic dynein[4–6]. We previously reported that calpain inhibition rescued defective phenotypes that are observed in *Lis1*$^{+/-}$ mice[7], suggesting that calpain inhibitors are a potential therapy for the treatment of lissencephaly. Here, we applied a novel blood-brain barrier (BBB) permeable calpain inhibitor, SNJ1945 for the treatment of lissencephaly[8–10].

Results

SNJ1945 rescued defective distribution of cytoplasmic dynein and membranous components in the cell and defective migration in *Lis1*$^{+/-}$ neurons. *In vitro* administration of SNJ1945 protected LIS1 from proteolysis, resulting in the augmentation of LIS1 levels in *Lis1*$^{+/-}$ mouse embryonic fibroblast (MEF) cells and leading to rescue of the aberrant distribution of cytoplasmic dynein and intracellular components including mitochondria and β-COP positive vesicles (Supplementary Fig. 1a–e). SNJ1945 also rescued defective distribution of cytoplasmic dynein and membranous components in human fibroblasts from an isolated lissencephaly sequence (ILS) patient, suggesting that SNJ1945 will be similarly effective in the human (Supplementary Fig.

2a–e). In addition, SNJ1945 improved neuronal migration of *Lis1*$^{+/-}$ cerebellar granular neurons (Supplementary Fig. 3). Notably, administration of even large doses did not result in obvious adverse effects on granular neurons (Supplementary Fig. 4). Oral administration of SNJ1945 to pregnant dams resulted in substantial increases of LIS1 levels in the brain of fetuses, as did oral administration directly to peri-natal offspring or adults (Fig. 1). Importantly, LIS1 levels increased in the brain three weeks after birth (Fig. 1c, f), indicating that indeed SNJ1945 passed through the BBB and inhibited proteolytic degradation of LIS1. Quantitative determination of drug concentrations in tissue homogenates via liquid chromatography-tandem mass spectrometry (LC-MS/MS) is commonly conducted using the standards. We measured the concentration of SNJ1945 in the brain using LC-MS/MS (Supplementary table 1). LC-MS/MS analysis indicated the brain distribution of SNJ 1945.

To demonstrate whether there was therapeutic benefit *in vivo*, we designed four different administration approaches (Fig. 2a): (1) intra-peritoneal injection starting at E9.5 (100 μg/g) followed by oral

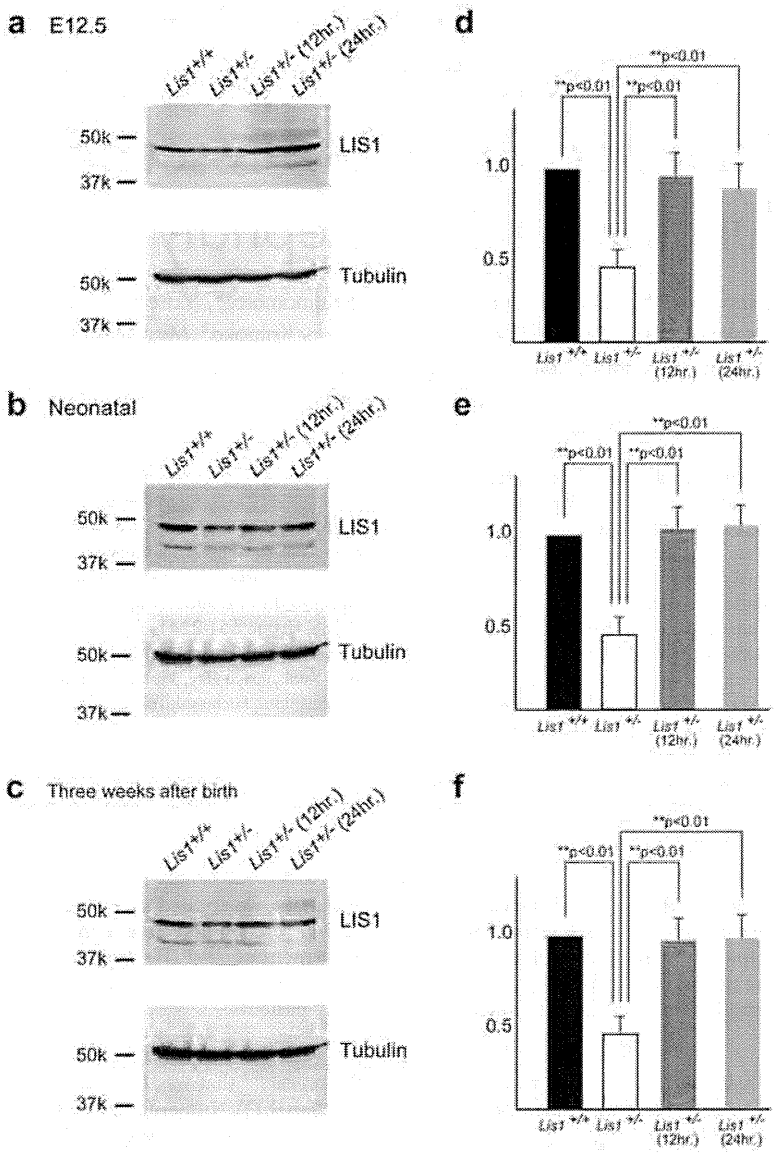

Figure 1 | Rescue of defective corticogenesis in *Lis1*$^{+/-}$ mice by SNJ1945. (a, b, c) Western blotting analysis of the brain after treatment of SNJ1945. Western blotting was performed on brain lysates after oral administration of SNJ1945. Time after oral administration is indicated at the top. Antibodies used for Western blots are indicated at the right of the Western blotting panels. Size maker and each molecular weight were shown at the left. Protein levels were normalized to tubulin beta-3 (Tubulin) as a control and are indicated at a graph (d, e, f). Statistical examination was performed by unpaired Student's *t*-test at 12 and 24 hrs after administration compared to *Lis1*$^{+/-}$, with **P < 0.01. Error bars in graphs were expressed as mean ± SEM. (a, d) SNJ1945 was taken orally as a mixture with food by pregnant dams at E12.5 (200 μg/g). At the indicated time, fetal brains were dissected and subjected to Western blotting analysis. We analyzed ten independent fetuses, and obtained reproducible results. One representative data set is shown. (b, e) SNJ1945 was gavage fed orally as a mixture with 0.5% carboxymethyl cellulose to neonatal pups (200 μg/g). At indicated time, brains of neonatal pups were dissected and subjected to Western blotting analysis. We analyzed ten independent pups. (c, f) SNJ1945 was taken orally as a mixture with food by *Lis1*$^{+/-}$ mice at three weeks after birth (200 μg/g). At indicated time, brain was dissected and subjected to Western blotting analysis. We analyzed ten independent mice, and obtained reproducible results. Note: LIS1 levels were increased to normal levels by 12 hrs. after oral administration. Importantly, SNJ1945 was effective in mice at three weeks, indicating that SNJ1945 is able to pass the BBB and protect LIS1 from degradation.

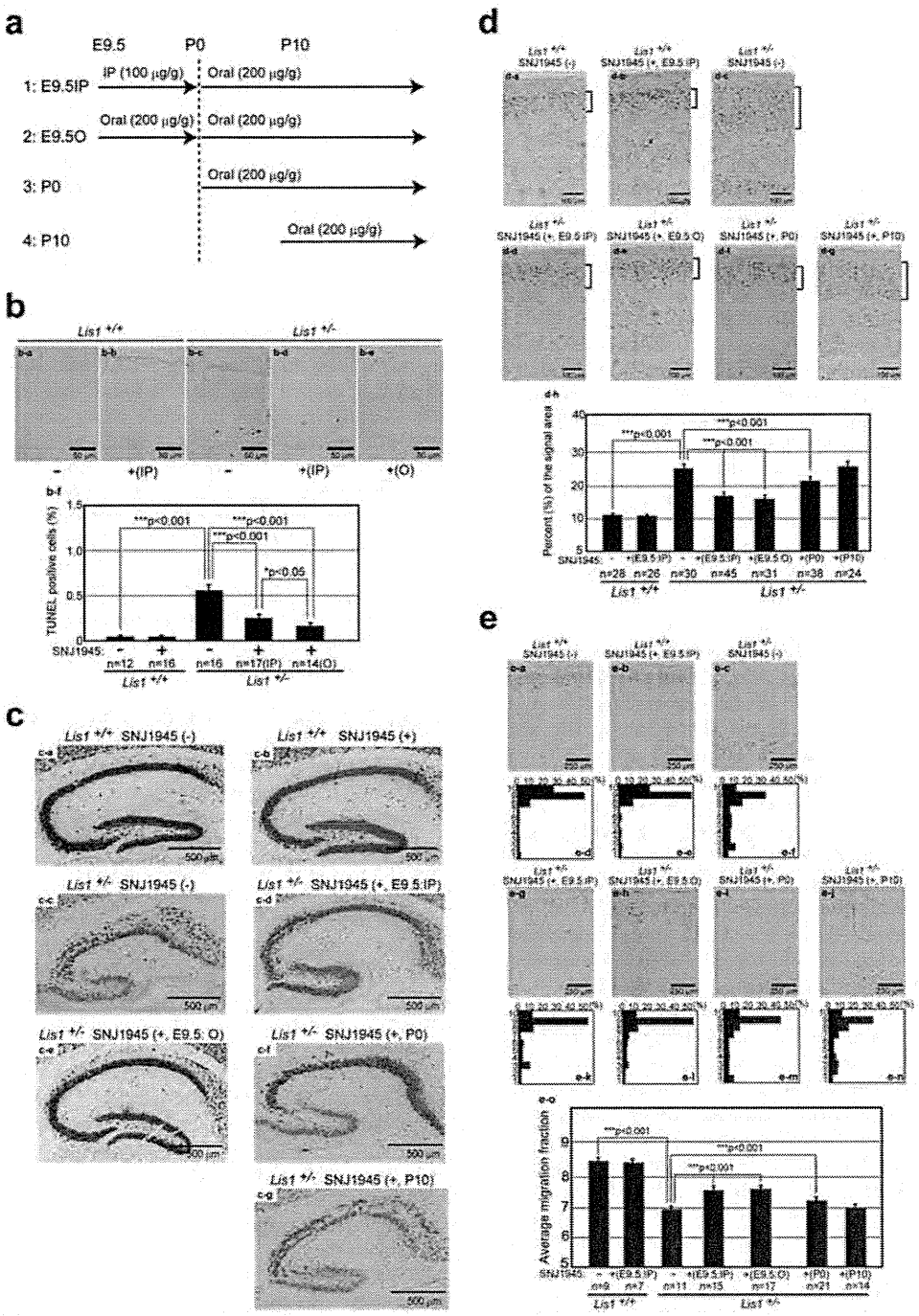

Figure 2 | Rescue of defective corticogenesis in *Lis1*$^{+/-}$ mice by SNJ1945. (a) Administration of SNJ1945 via four protocols (see methods). (b) Apoptotic cell death was examined by TUNEL staining at E15.5. One representative data set is shown (b-a, b, c, d, e). Histogram plots of the relative frequency of TUNEL positive cells to the total number of cells are shown at the bottom (b-f). The staining patterns are representative of different experiments as indicated at the bottom of the panel. *n* is the number of examined brains. Statistical examination was performed by unpaired Student's *t*-test. Error bars in graphs were expressed as mean ± SEM. (c) Neu-N staining of mid-sagittal sections of the hippocampus is shown. Severe cell dispersion and splitting of CA3 region were observed in the *Lis1*$^{+/-}$ mouse hippocampus (c-c), which improved by the administration of SNJ1945 (c-d, e, f, g). Other examples are shown in Supplementary Figure 6. (d) Cortical phenotypes were examined using a layer specific maker, Brn-1 (layer 2 and 3). The distribution of Brn-1 positive cells is indicated at the right side of each panel (d-a, b, c, d, e, f, g). Brn-1 positive cells were more dispersed in the *Lis1*$^{+/-}$ mouse (d-c). Quantitation of the thickness of Brn-1 positive cells is summarized at the bottom (d-h). The staining patterns are representative of different experiments as indicated at the bottom of the panel. The dispersion of Brn-1 positive cells is improved by the administration of SNJ1945. *n* is the number of examined brains. Statistical examination was performed by unpaired Student's *t*-test. Values in graphs were expressed as mean ± SEM. (e) BrdU birthdating analysis revealed neuronal migration defects in the *Lis1*$^{+/-}$ mouse. Quantitation of the thickness of BrdU positive cells is summarized at the bottom (e-o). The distribution of BrdU labeled cells in each bin that was equally divided the cortex from ML to SP. The staining patterns are representative of five different experiments. The shift downward toward the ventricular side as *Lis1* was disrupted. Treatment of SNJ1945 rescued neuronal migration to more superficial (later born and further migrating) areas.

administration after birth (200 μg/g), (2) oral administration starting at E9.5 (200 μg/g) followed by oral administration after birth (200 μg/g), (3) oral administration starting in the peri-natal period (200 μg/g) and (4) oral administration starting ten days after birth (200 μg/g). We previously reported a mild reduction of the density of cells in the neocortex of the *Lis1*$^{+/-}$ mice[11]. At E15.5 when later migrating neurons are generated, a significant acceleration of apoptotic cell death in the ventricular zone was observed[11]. These results prompted us to investigate apoptotic cell death during corticogenesis by TUNEL staining at E15.5 (Fig. 2b). In *Lis1*$^{+/-}$ mice, apoptotic cell death was clearly increased[11]. In contrast, administration of SNJ1945 suppressed apoptotic cell death in *Lis1*$^{+/-}$ mice (Fig. 2b). We also examined whether administration of SNJ1945 had any effects on mitotis, since LIS1 is essential for mitotic cell division[12] and neuroepithelial stem cell proliferation[13]. At E13.5, we performed BrdU pulse labeling and found that BrdU incorporation was not significantly different among the five groups (Supplementary Fig. 5), indicating that there was no measureable effect of SNJ1945 on proliferation of neuroepithelial stem cells. We next examined the effect of SNJ1945 on the cortical and hippocampal layering of neurons. *Lis1*$^{+/-}$ mice exhibited laminar splitting and discontinuities of pyramidal cells in the CA3 and CA2 region of the hippocampus (Fig. 2c), as we previously demonstrated[12]. After administration of SNJ1945 *in utero*, *Lis1*$^{+/-}$ mice also displayed splitting and discontinuities in the pyramidal cell layer of the hippocampus, but these defects were markedly improved compared with untreated mice (Fig. 2c and Supplementary Fig. 6a–c). To examine cortical lamination, we analyzed Brn-1 immunoreactivity, to label neurons of layer 2 and 3[14]. In *Lis1*$^{+/-}$ mice, Brn-1 positive cells (which migrate at later stages) exhibited a broader distribution compared to *Lis1*$^{+/+}$ mice. Administration of SNJ1945 resulted in more tightly packed layer 2/3 neurons in *Lis1*$^{+/-}$ mice (Fig. 2d), suggesting that neuronal migration in the cortex was also improved by the inhibition of LIS1 degradation. In both the hippocampus and cortex, oral administration starting postnatally was also partially effective but less effective than when treatment started *in utero* (Fig. 2c, d and Supplementary Fig. 6a–c). To confirm that the morphological defects observed in *Lis1*$^{+/-}$ mice were improved by SNJ1945 treatment, we performed quantitative BrdU birthdating analysis. In *Lis1*$^{+/-}$ mice, the distribution of labeled cells was shifted downward toward the ventricular zone in the cortex, and BrdU-labeling was more diffusely localized (Fig. 2e), as we previously demonstrated[12]. These migration defects associated with the disruption of *Lis1* were partially rescued in the presence of SNJ1945 (Fig. 2e). Thus, we concluded that oral administration or intra-peritoneal injection of SNJ1945 *in utero* are effective in rescuing defective neuronal migration. Importantly, oral administration commencing postnatally was also partially effective, resulting in improvement of brains structure including hippocampus and cortex. In contrast, oral administration starting ten days after birth did not result in any obvious benefits, suggesting that some fraction of neurons was still migrating at the time of birth[15], which was essentially complete by ten days after birth.

SNJ 1945 partially rescued impaired motor behavior. *Lis1*$^{+/-}$ mice displayed abnormal behavior and impaired spatial learning[7,16]. Therefore, we examined whether administration of SNJ1945 to *Lis1*$^{+/-}$ mice is effective in improving motor behavior compared to untreated *Lis1*$^{+/-}$ mice. Body weight and temperature were not significantly different among groups, (Supplementary Table 1). As shown in our previous report, *Lis1*$^{+/-}$ mice exhibited shorter wire-hang latency compared with wild-type mice, and this decreased latency was rescued by SNJ1945 treatment (Fig. 3a). This improvement was most significant in the group in which treatment was started from fetal times (*Lis1*$^{+/-}$E9.5). Next, we examined rotarod performance. The latency to fall for the SNJ1945-minus group was significantly less than wild type mice, as we previously reported[7]. Impaired performance on the rotarod test was significantly improved in the SNJ1945-treated groups (Fig. 3b, Supplementary Fig. 7). This functional improvement was also observed not only in the *Lis1*$^{+/-}$E9.5 group, but also in the *Lis1*$^{+/-}$P0 group, in which treatment was started perinatally. In our previous report, we demonstrated that *in utero* treatment of a calpain inhibitor from fetal stages improved gait performance. Consistent with this finding, administration of SNJ-1945 significantly improved the percent of stride in swing and swing to stance ratios in the *Lis1*$^{+/-}$E9.5 group (Fig. 3c). Most importantly, these improvements were also observed in the *Lis1*$^{+/-}$P0 and *Lis1*$^{+/-}$P10 groups. The Porsolt forced swim test is the most commonly used test for assessment of depression-like behavior in animal models. Mice were placed in an inescapable cylinder half-filled with water to induce the behavioral state of despair. We measured periods of immobility, in which longer immobile times indicated higher degrees of despair (Fig. 3d). We found that *Lis1*$^{+/-}$ mice displayed significantly increased immobile times compared with controls. SNJ1945 treated *Lis1*$^{+/-}$ groups displayed immobile times intermediate between *Lis1*$^{+/+}$ mice and *Lis1*$^{+/-}$ mice. In particular, improvement close to normal levels was observed in the *Lis1*$^{+/-}$E9.5 group. Our findings suggest that SNJ1945 treatment can rescue depression-like status in *Lis1*$^{+/-}$ mice. It is possible that the rescue of this behavioral abnormalities in *Lis1*$^{+/-}$ mice by SNJ1945 treatment results from the improved coordination of motor function by SNJ1945. Another possibility is that treatment of SNJ1945 rescued depression-like status in *Lis1*$^{+/-}$ mice, which led to improvement of behavioral performance.

Small-animal positron emission tomography (PET) was used for evaluation of brain functional improvement by SNJ1945 treatment. We further addressed whether the rescue of defective behaviors in *Lis1*$^{+/-}$ mice by SNJ1945 treatment was associated with the improvement of brain function. Small-animal imaging studies using PET have been increasingly applied in murine models for drug discovery[4]. We here employed PET imaging with 2-deoxy-2-^{18}F-fluoro-D-glucose (FDG) to evaluate brain neural activity based on glucose metabolism[17]. We found aberrations in FDG uptake patterns in *Lis1*$^{+/-}$ mice that responded to SNJ1945 treatment. PET scans with FDG in human lissencephaly patients demonstrated two layers in the cerebral cortex that could be differentiated based on metabolic activity[18], corresponding to the inner cellular layer of the lissencephalic cortex and the molecular, outer cellular, and cell-sparse layers, respectively[18]. In our PET imaging, we were not able to observe such a layered pattern in *Lis1*$^{+/-}$ mice due to the limitation of spatial resolution (Fig. 4a). *Lis1*$^{+/-}$ mice displayed similar glucose utilization in the cortex, hippocampus and cerebellum compared to wild type mice (Supplementary Fig. 8). Interestingly, we found significantly reduced glucose utilization in the basal forebrain, hypothalamus and amygdala (Fig. 4a, b). Most importantly, these reductions in FDG uptake were reversed by the treatment with SNJ1945 (Fig. 4a, b). The recovery of glucose metabolism is consistent with the improvement of behavioral performance by treatment with SNJ1945.

SNJ1945 improved neural network formation and facilitated clustering of GABA receptors in amygdala. Because behaviors and brain metabolism are highly linked to the interactive dynamics of neural circuits and synaptic formation in the brain, it is possible that SNJ1945 also rescued defective network formation and synaptogenesis in *Lis1*$^{+/-}$ mice, which might account for the functional improvement of behavioral performance and FDG uptake even without migratory rescue (such as after treatment commencing at P10). To address this question, we injected *TdTomato*[19] into embryos to visualize neural networks at E16.5[20]. In particular, we have focused on neural networks in amygdala (Fig. 5a). While there were no notable differences in the size of the soma, *Lis1*$^{+/-}$ mice displayed a striking simplification of dendrites compared to *Lis1*$^{+/+}$ mice

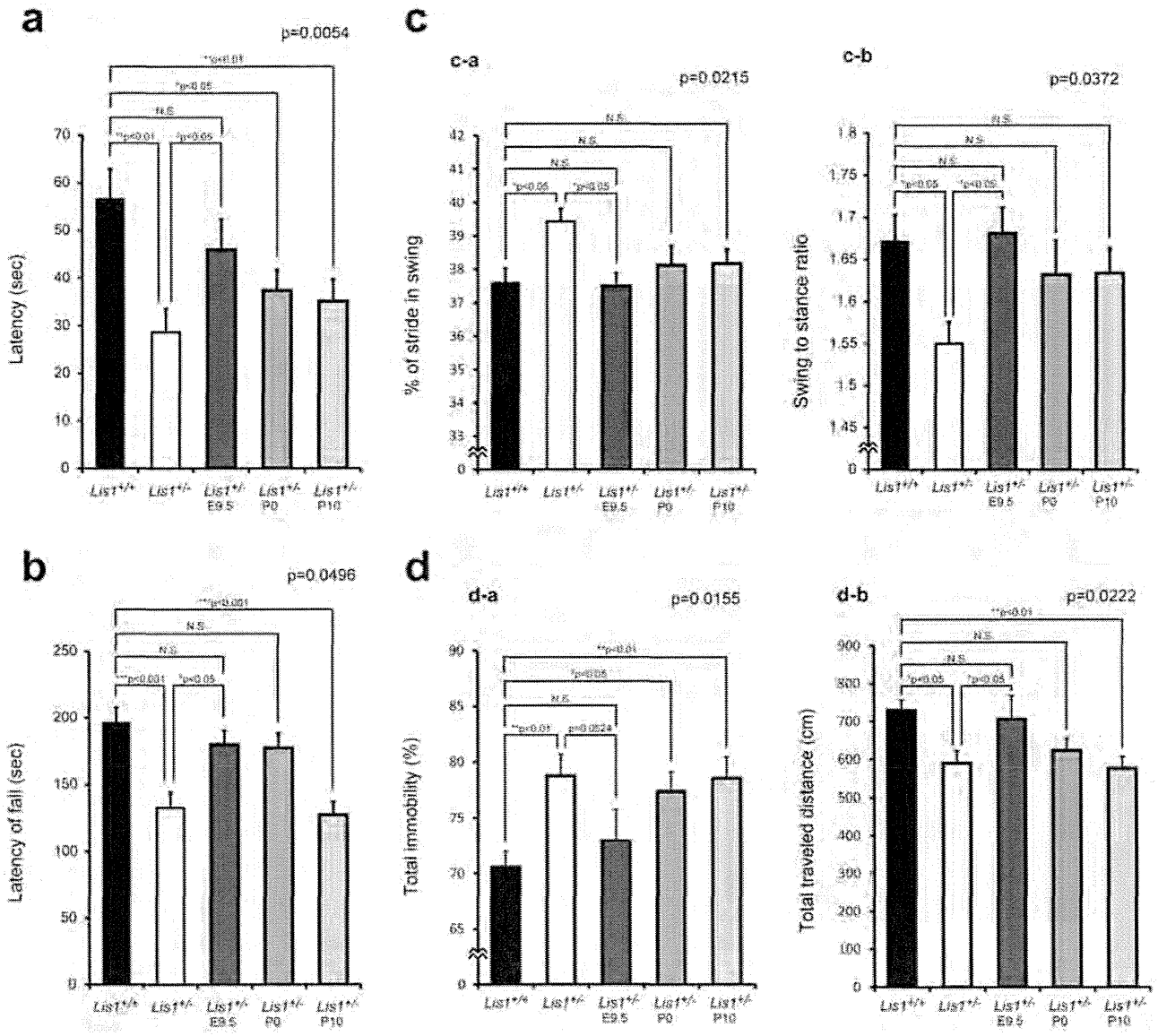

Figure 3 | Mouse behavior analysis. We examined behavioral performance of *Lis1*$^{+/+}$ mice, *Lis1*$^{+/-}$ mice and *Lis1*$^{+/-}$ mice with SNJ1945 treatment after the administration protocol described in Fig. 2a. *Lis1*$^{+/+}$, wild type mice, *Lis1*$^{+/-}$; *Lis1*$^{+/-}$ mice without treatment, *Lis1*$^{+/-}$E9.5; *Lis1*$^{+/-}$ mice with oral administration from E9.5 (200 μg/g) followed by oral administration after birth (200 μg/g), *Lis1*$^{+/-}$P0; *Lis1*$^{+/-}$ mice with oral administration from peri-natal period (200 μg/g) *Lis1*$^{+/-}$P10; *Lis1*$^{+/-}$ mice with oral administration from ten days after birth (200 μg/g). P-values are shown at the upper parts of bars. Statistical analysis was conducted using Stat View (SAS institute). Data were analyzed by one-way ANOVA. Error bars in graphs were expressed as mean ± SEM, and P-values indicated a group effect by one-way ANOVA. Statistical significance was defined as $^{*}P < 0.05$, $^{**}P < 0.01$ and $^{***}P < 0.001$. (a) Wire hang test. *Lis1*$^{+/-}$ mice displayed clear shorter latency to fall in the wire hang test. Administration of SNJ1945 improved hanging time. (b) Examination of motor function by the rotarod test. Time spent balanced on top of the rotating rod was measured across six test trials. The graph indicates summation of the latency through the six test trials. Significant differences between *Lis1*$^{+/+}$ mice and *Lis1*$^{+/-}$ mice ($^{***}P < 0.001$) were observed. SNJ1945 treatment resulted in improvement of rotarod performance but was less effective with the delayed treatment. Importantly, treatment starting at P0 was still effective. (c) Gait analysis using the DigiGait treadmill apparatus: percent of stride in swing (c-a) and swing to stance ratio (c-b) are shown. *Lis1*$^{+/-}$ mice with SNJ1945 treatment displayed improvement of gait parameters. Importantly, treatment from P10 was still effective, suggesting SNJ1945 can improve brain function after much of development has finished. (d) Porsolt swimming test. Immobility (d-a) and distance traveled (d-b) are shown at Day 2.

(Fig. 5b, c, d, Supplementary Fig. 9). Branching and length of each branch were decreased to approximately 29% and 27%, respectively. Importantly, the poor development of dendritic arbors and decreased each length in *Lis1*$^{+/-}$ mice were rescued by SNJ1945 treatment (Fig. 5b, c, d, Supplementary Fig. 9), suggesting that neurons in the amygdala partially maintain plasticity, and proper network formation was facilitated by the treatment after P10.

The amygdala has an important role in processing emotional information[21–23]. Inappropriate processing within the amygdala is thought to induce anxiety disorders. Benzodiazepines, which act specifically on $GABA_A$ receptors, are commonly used as anxiolytics. This implies that GABAergic synapses within the amygdala may have an important role in inducing or compensating for these disorders. $GABA_A$ receptors are clustered at synaptic sites to achieve a